A study of packaging schemes for SMS optical fibre temperature sensor

R. F. ADIATI[a,b], A. M. HATTA[a]
[a]*Photonics Engineering Laboratory, Department of Engineering Physics, Institut Teknologi Sepuluh Nopember, Surabaya, Indonesia*
[b]*Department of Physics, IPB University, Bogor, Indonesia*

While optical fibre-based sensors are well-developed and applied at various measurements, it is fragile. Therefore, packaging of the sensor is an important aspect. In this paper, packaging schemes for singlemode-multimode-singlemode optical fibre are observed numerically and experimentally. The effect of material variation to the sensitivity of temperature sensor is observed between 25-100 °C. Packaging thickness and shape variation is also taken into consideration. Both intensity-based interrogation and wavelength shift method show that the sensitivity of the sensor increases when packaging is applied, compared to the bare SMS sensor. The application of PTFE as packaging increases the sensitivity of SMS sensor, from 0.0103 dB/°C to -0.0590 dB/°C, about 5.7 times higher.

(Received August 21, 2020; accepted April 7, 2021)

Keywords: Optical Fibre Sensor, Temperature Sensor, SMS Fibre Structure, Packaging

1. Introduction

Optoelectronics technologies, such as optical fibre sensor has been vastly developed since its first establishment. Currently, optical fibre sensors are applied for various measurements e.g. strain [1], temperature [2], refractive index [3], position, vibration [4] [5], electric and magnetic field, displacement [6], also as biochemistry sensor [7]. The main advantage of optical fibre sensors is its dielectric property. It also can withstand high temperature or corrosive environment. Moreover, these sensors are small in size, have a low energy consumption, and compatible with both remote sensing and communications system [8].

Several approaches are applied for optical fibre sensors, such as evanescent field [9], taper effect [10], Bragg resonance [11], and multimode interference (MMI) [12]. Bragg resonance inside Fibre-Bragg grating (FBG) is widely used as strain and temperature sensor because of these characteristic: 1) intrinsic sensing, 2) able to be directly fabricated into the optical fibre without changing its diameter, 3) the signal is in wavelength domain and applicable for wavelength division multiplexing (WDM) technique if it is used for multiple detections [13]. However, the MMI effect observed in optical fibre singlemode-multimode-singlemode (SMS) structure also comes as a promising technique for measurement and signal processing [14] [2].

Compared to FBG, the SMS structure provides sensitive measurement while maintaining easy fabrication, low-cost, and stable configuration [15]. Through intensity-based interrogation, SMS sensors are able to do simultaneous measurements [16] [17].

Previous researches demonstrated the use of SMS fibre structure as temperature sensors, for both step-index multimode [18] and the graded-index ones [19]. To enhance the performance of the sensor, structural modifications were made, such as the addition of anti-polarization fibre [1], no-core fibre [20], twisted multimode fibre [16], or doped fibres [14]. Another way to enhance the performance, i.e. the sensitivity of the SMS fibre sensor is the addition of packaging, which also functions as mechanical protection for the fragile nature of optical fibres.

The application of packaging increases sensor performance. For examples in FBG sensor, nickel and steel used as packaging [21], also some polymers applied in temperature and strain measurement such as Polypropylene, epoxy, quartz glue, and Polymethyl-methacrylate [22] [23]. Polymers are mainly used to avoid electromagnetic interference while increasing sensor sensitivity. Some reports about packaging in SMS sensor also showed various material such as steel and aluminium [24], or Polyurethane-acrylate as multimode cladding [25]. However, most of the reports indicated a very specific range of operation for the sensors. For example, the sensor had around 10 °C range of operation [22] [2] or had different responses for a different range of temperature [25]. Others had wider range, around 50-75 °C [23] [24] [17].

In this paper, packaging schemes for SMS fibre sensor are observed numerically and experimentally. The packaging is designed to be applied in structural health monitoring, so the material response to a harsh environment is considered. Steel, aluminium, and Polytetrafluoroethylene (PTFE) are selected as packaging material. Also considering the proposed application, the simulation and experiment are conducted in a wide range

of temperature, that is 25-100 °C.

There have been some reports about the application of PTFE as a packaging of optical fibre sensors. FBG temperature sensor was packaged with steel tube casing, with manganese steel alloy as the substrate in [26], resulting in 6.64 pm/°C sensitivity. In [27], PTFE effect was simulated as FBG packaging, while taking into consideration the phase transitions of PTFE in different temperatures. The sensitivity obtained was 0.3 nm/°C. In [28], PTFE was used as a coating of FBG temperature sensor, with various thickness and applied using electrostatic spray technique. The sensitivity of Teflon coated FBG reached 12.85 pm/K from -196 °C to 25 °C and 14.04 pm/K from 25 °C to 800 °C, three times as large as that obtained with the regular FBGs. Another report used capillary encapsulating PTFE tube for FBG with two endpoints fixed [29] and obtained sensitivity about 23.4 times higher than bare FBG temperature sensor.

The material variation and optical fibre parameters are simulated numerically, in which the best result is investigated through a series of experiment. Both intensity interrogation and wavelength shift method are utilized. The effect of the packaging to the sensitivity of the optical fibre temperature sensor then calculated.

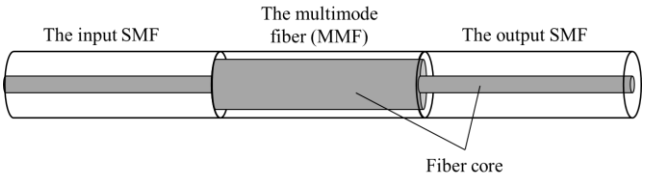

Fig. 1. The schematics of singlemode-multimode-singlemode fibre structure

2. Method

The SMS fibre structure is a certain length of multimode fibre spliced with singlemode fibre on both ends as shown in Fig. 1. The multimode interference (MMI) phenomenon occurring inside the multimode fibre (MMF) section, forming maxima and minima interference patterns along the propagation length. This particular phenomenon enables the SMS fibre structure to be applied as a sensor at certain MMF length. In the numerical analysis, the optimum length of the MMF section is calculated. Then, the effect of packaging on the output power of the sensor is calculated. In the experimental analysis, the selected MMF length and packaging scheme is characterized.

2.1. Numerical analysis

The numerical calculation of the SMS sensor output is based on the modal propagation analysis (MPA) [30], which describes the propagation of light inside an SMS structure. The calculation of MPA is based on how light from input singlemode fibre (SMF) has only one fundamental mode with E(r,0) field profile, then this mode will be divided into some linearly polarized mode with field profile Fm(r) the moment it enters the MMF section. The mathematical expression for the field distribution is [30]:

$$\int_0^\infty |E(r,0)|^2 \, r dr = \int_0^\infty |F_m(r)|^2 \, r dr \quad (1)$$

$$E(r,0) = \sum_{m=1}^{M} c_m F_m(r) \quad (2)$$

where c_m is the excitation coefficient for each m modes estimated by:

$$c_m = \frac{\int_0^\infty E(r,0)\, F_m(r)\, r dr}{\int_0^\infty F_m(r)\, F_m(r)\, r dr} \quad (3)$$

The electric field distribution varies during the propagation of light, affected by the distance z,

$$E(r,z) = \sum_{m=1}^{M} c_m F_m(r) \exp(i\beta_m z) \quad (4)$$

where

r : core radius of MMF
n_c : refractive index of the core
n_{cl} : refractive index of the cladding
λ : wavelength
c_m : excitation coefficient of mode number m

$F_m(r)$: field profile of mode number m
β_m : propagation constant
Z : propagation length

Equation (4) shows that the field profile of each mode and propagation length (z) affects the electric field distribution. Assumed that lead-in and lead-out SMFs are identical, the coupling loss Ls of SMS optical fibre structure stated by:

$$L_s(z) = 10 \log_{10} \left(\left| \sum_{m=1}^{M} c_m^2 \exp(i\beta_m z) \right|^2 \right) \quad (5)$$

The output power P_{out} (dB) at the connection between MMF end and SMF lead-out can be calculated with:

$$P_{out} = 10 \log_{10} \frac{\left| \int_0^\infty E(r,z) E_0(r) r dr \right|^2}{\int_0^\infty |E(r,z)|^2 r dr \int_0^\infty |E_0(r,z)|^2 r dr} \quad (6)$$

MMI phenomena happening in the MMF can be affected by external stimuli such as temperature changes. The temperature inflicts changes in SMS fibre structure parameters e.g. length, core radius, and refractive index, where according to the MPA analysis, can affect the output power of the SMS fibre sensor. The first simulation is to find the optimal length of MMF section so the propagation length is in accordance with maxima pattern.

The principle of temperature measurement as mentioned before, is the change of fibre parameters due to external temperature change. The change depends on the

coefficient of thermal expansion (CTE, α) and thermo-optic coefficient (ξ) of the silica fibre, where $\alpha=5\times10^{-7}$/°C and $\xi=6.9\times10^{-6}$/°C [2]. When packaging is applied, the CTE of the packaging material becomes important because the difference between aforementioned parameter and the CTE of silica material is causing an axial strain due to thermal expansion as follows [31]:

$$\varepsilon = (\alpha_f - \alpha_p)\Delta T \quad (7)$$

The change of optical fibre parameters are described in the following equations [14]:

$$\Delta L = L\varepsilon + \alpha_{fibre} L\Delta T \quad (8)$$

$$\Delta r = -\sigma r\varepsilon + \sigma r\Delta T \quad (9)$$

$$\Delta n = -p_e\varepsilon + \beta n\Delta T \quad (10)$$

where ΔL is an MMF length variation, Δr is core radius variation, σ is the Poisson ratio, Δn is the refractive index variation of core and cladding, and p_e is the effective strain-optic coefficient.

Substituting eq. (7) into eq. (8-10), it can be obtained:

$$\Delta L = L(\alpha_f - \alpha_p)\Delta T + \alpha_p L\Delta T + \alpha_f L\Delta T \quad (11)$$

$$\Delta r = -\sigma r(\alpha_f - \alpha_p)\Delta T + \sigma r\Delta T \quad (12)$$

$$\Delta n = -p_e(\alpha_f - \alpha_p)\Delta T + \beta n\Delta T \quad (13)$$

Table 1. Approximated properties of selected materials

Material	**Coefficient of Thermal Expansion (/°C)**	**Thermal conductivity (W/m K)** [32]
Silica (optical fibre)	5×10^{-7} [31]	1.3
Steel	$1{,}1 \times 10^{-5}$ [31]	14.4
Aluminium	$2{,}36 \times 10^{-5}$ [33]	237
Polytetrafluoroethy-lene (PTFE)	$1{,}24 \times 10^{-4}$ [34]	0.25

Equations (11) to (13) show how different packaging material results in different parameter changes. Thermo-optic effects of the fibre materials and its packaging affect the propagation constants of the fibre modes involved in the modal interferences, and eventually produces different SMS power output [2]. The simulation calculates different responses for three packaging materials shown in Table 1 through intensity-based interrogation method [18] and wavelength shift method.

Taken into account that the proposed use of this optical fibre temperature sensor is for structural health monitoring, in the selection process of the material, several factors are considered: chemically inert material, good thermal conductor, and has been used as optical fibre packaging in previous experiments. Thermal conductivity affects the rate of heat conducted by the packaging material to the optical fibre sensor, directly related to the time response of the sensor.

2.2. Experiment

The first step of the experimental stage is the fabrication of the SMS fibre sensor. The MMF length selected is 43 mm, giving the best linearity based on the simulation result. The MMF was spliced to SMF pigtails. After the fabrication, the sensor was characterized using intensity-based interrogation method. The output of the SMS fibre sensor was measured at a temperature range of 25-100 °C with 5 °C increments. Set up for this method is shown in Fig. 2. The optical light source used was Joinwit JW3019 laser diode, with 1550 nm wavelength and -6 dBm power. Thorlabs PM100 photodiode functioned as a light detector. The heat source was hotplate, which was manually controlled with an accuracy of 1˚C, and checked regularly with an infrared thermometer.

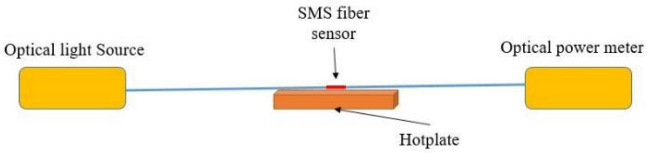

Fig. 2. Set up for intensity-based characterization (color online)

After the bare SMS sensor characterization, the next step is packaging installation. The PTFE sheet was cut into bar-shape, and there were 2 shape variation, i.e. one-sided packaging and two-sided packaging, consecutively shown in Fig. 3. To install the packaging, a small v-shaped groove was cut into the PTFE material to embed the fibre sensor, epoxy resin was used as glue material. In the 2-sided packaging, the v-groove facilitated direct contact between two PTFE sheets.

In the wavelength shift method, the transmission spectra of the optical fibre sensor were measured between 1500-1600 nm with set up shown in Fig. 4. For the light source, the Oceanoptics HL-2000-LL tungsten halogen, with 360-2400 nm wavelength was used, while the detector was OtoPhotonics Spectrasmart. The results of this method are shown as intensity vs. wavelength graph.

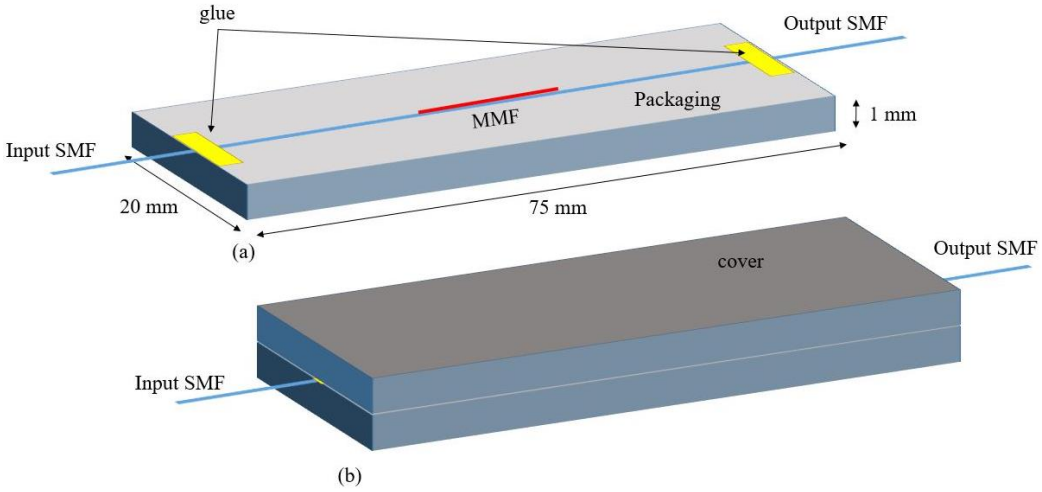

Fig. 3. Design of optical fibre sensor packaging; (a) one-sided packaging, (b) two-sided packaging (color online)

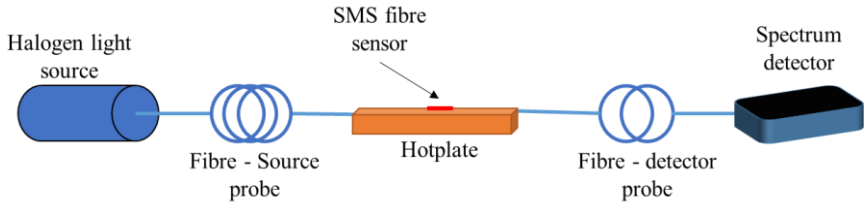

Fig. 4. Set up for transmission spectrum characterization (color online)

3. Results and discussions

3.1. Simulation results

The simulation was conducted based on the numerical analysis described in section 2.1. The propagation of light was calculated for every mode number according to multimode interference. Then, the power output was presented as the function of wavelength, temperature, and type of packaging.

Fig. 5 shows how wavelength shift was used as an analysis of sensor sensitivity. The sensitivity of SMS fibre sensor can be expressed as the displacement of wavelength per unit temperature, in this case, between 1500 and 1600 nm. In this calculation, multimode fibre (MMF) length was 43 mm, as selected from the best response given by the MMF length between 42.5 and 43.5 mm. This particular wavelength ranges and MMF length was selected because it showed the most linear result in intensity interrogation method among other wavelength and fibre parameters (see Fig. 6).

The bare SMS sensor was the default value, where the peak was at 1545.34 nm. The rise of temperature shifted the output power response to the longer wavelength (red shift). At 100 °C temperature raise, the wavelength peak was at 1546.32 nm. Meanwhile, the presence of packaging induced the shift to lower wavelength (blue shift). The new peaks for steel, aluminium, and PTFE were 1544.27 nm, 1541.82 nm, and 1523.005 nm consecutively. The simulated value of wavelength shift is shown in Table 2.

Table 2. Simulated value of sensor sensitivity using wavelength shift

Packaging type	Simulated sensitivity (pm/°C)
Bare sensor	9,85
Steel packaging	-10,64
Aluminium packaging	-35,15
PTFE packaging	-223,35

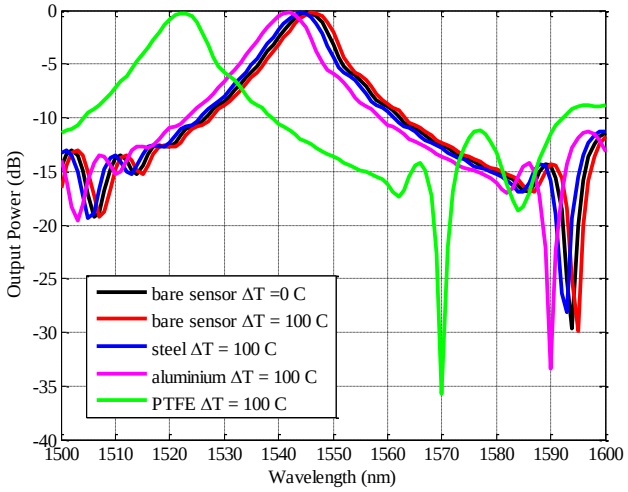

Fig. 5. Simulation result: the power output response of SMS fibre structure temperature sensor for 1500 - 1600 mm wavelength at various packaging material (color online)

The different CTE values of packaging material give different values of wavelength shift. The higher CTE value, the more axial strain is induced by the temperature change, resulting in a higher wavelength shift. The blue shift indicates that the silica fibre material is overcompensated by the packaging.

The sensitivity of the PTFE-packaged sensor is the highest among other packaging materials. PTFE characteristic as a thermoplastic polymer with high-temperature conductivity is also an advantage compared to metal packaging. Because it cannot be affected by magnetic interference, PTFE is an excellent packaging material for optical fibre sensor in several applications.

Another way to express the sensitivity of optical fibre sensor is by using intensity interrogation method. The sensitivity of the sensor can be expressed as the power output change per unit temperature or the gradient of power vs. temperature graph. The graph is shown in Fig. 6.

As shown in Fig. 6, there is a consistence of increasing or decreasing response for all sensors, with or without packaging. In the case of raised temperature at a bare sensor, the response has a positive gradient, and the use of packaging causing negative gradient. When there is no packaging, the axial strain affecting fibre parameters depends only to the CTE of fibre material (equations (8) to (10)). The power output calculated increases with temperature, having a positive slope, as opposed to when packaging is applied. The sensitivity of the sensors is listed in Table 3. For PTFE-packaged sensor, the sensitivity is 0.1050 dB/°C, about 9.4 times higher than the bare sensor, which sensitivity is 0.011dB/°C.

Table 3. Simulated value of sensor sensitivity using intensity interrogation method

Packaging type	Simulated sensitivity (dB/°C)
Bare sensor	0.0112
Steel packaging	-0.0123
Aluminium packaging	-0.0275
PTFE packaging	-0.1050

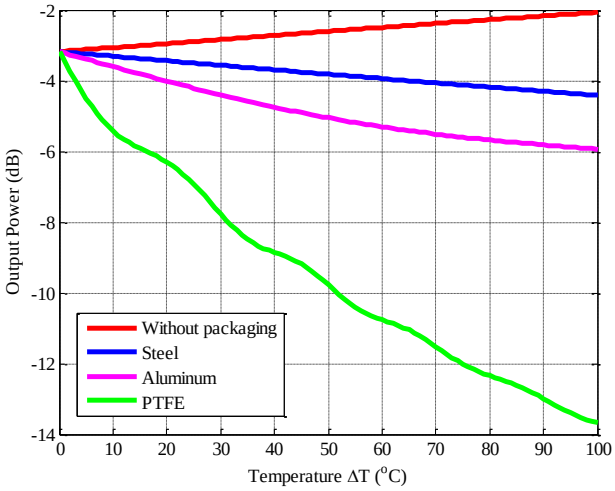

Fig. 6. Simulation result: the power output response of SMS fibre structure temperature sensor for 100 °C temperature change at various packaging material (color online)

3.2. Experimental results

a. Intensity interrogation method

The fabrication of SMS fibre structure was the first step of the simulation. The singlemode fibre pigtails were connected to 43 mm multimode fibre using fusion splicer. The characterization of the sensor was conducted using intensity-based interrogation method at the temperature between 25 °C - 100 °C, with 5 °C increments. The light source was a diode laser of 1550 nm wavelength and -6 dBm power. The sensor was characterized before and after the installation of packaging. The SMS structure of optical fibre was glued to PTFE using epoxy resin as shown in Fig. 7. The figure shows one-sided packaging, which characterization result is in Fig. 8 and Table 4.

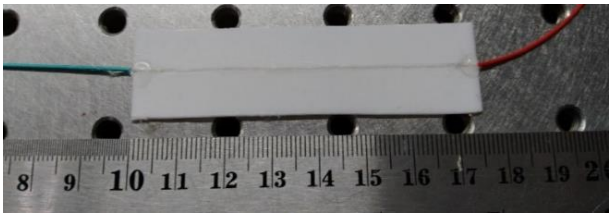

Fig. 7. SMS fibre sensor with one-sided PTFE packaging

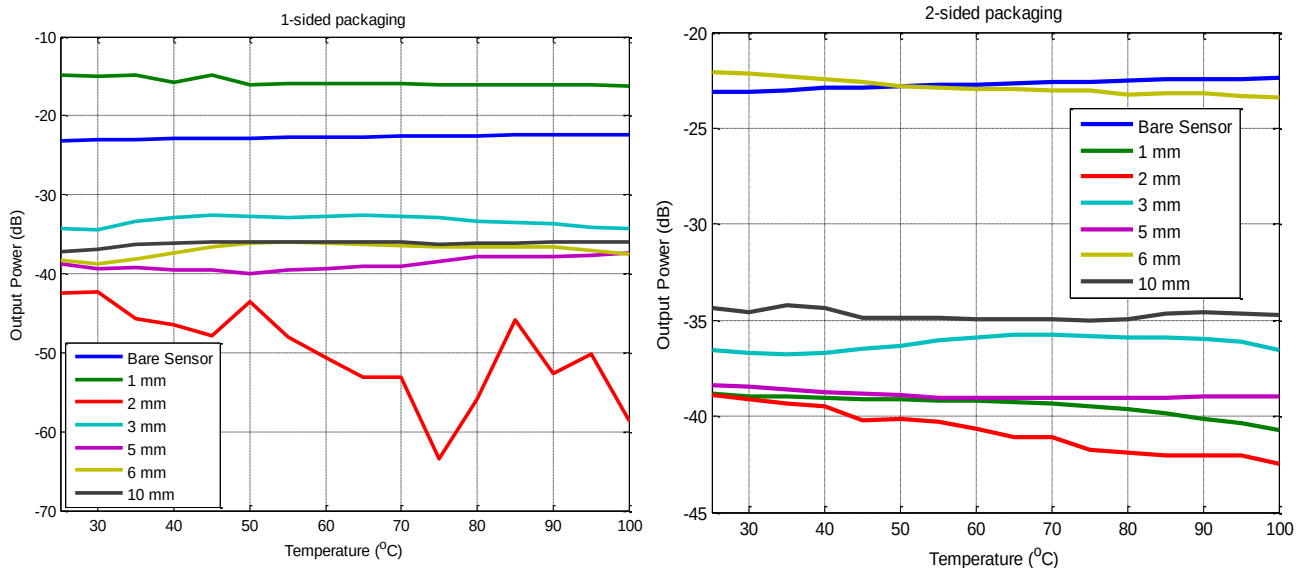

(a) (b)

Fig. 8. Experiment result: the output response of SMS fibre temperature sensor with (a) one-sided packaging and (b) two-sided packaging at various temperature and thickness, epoxy resin as glue (color online)

Table 4. The sensitivity of PTFE-packaged SMS fibre temperature sensor

Type of PTFE Packaging	Thickness	Sensitivity (dB/°C)		
		Simulation	Experiment	Remarks
Bare Sensor	-	0.0110	0.0102	
One-sided packaging	1 mm	-0.1050	-0.0179	
	2 mm	-	-0.2155	highly fluctuates
	3 mm	-	-0.0471	for 65°C-100°C
	5 mm	-	-0.0437	for 25°C-50°C
	6 mm	-	-0.0352	for 55°C-100°C
	10 mm	-	0.0176	
Two-sided packaging	1 mm	-	-0.0246	
	2 mm	-	-0.0482	
	3 mm	-	0.0281	for 35°C-70°C
	5 mm	-	-0.0223	for 25°C-55°C
	6 mm	-	-0,0181	
	10 mm	-	-0,0052	for 45°C-75°C

Similar to the simulation result in Fig. 6, the sensitivity of the sensor can be calculated as the gradient of the response lines. It can be examined that the gradient is positive for the bare sensor, with a sensitivity of 0.0102 dB/°C. The response for a PTFE-packaged sensor has different values of sensitivity depends on the thickness, as shown in Table 4. For one-sided packaging, Fig. 8(a), the best result is obtained at 1 mm packaging thickness. As examined, the response for 2 mm packaging has very high fluctuation, and a linear result is only obtained in a certain range for 3, 5, and 10 mm thickness.

The results show that the sensitivities of all measurements are lower than the simulated values. This can be caused by an unbalanced expansion of PTFE material; also the packaging is only present on one side and the top side of the sensor is not protected. Direct observation indicates that the high difference of CTE between the optical fibre and PTFE, combined with epoxy resin locking the material expansion, causing the bending of PTFE material as shown in Fig. 9. It is also observed that the current design with bar shape does not accommodate uniform strain transfer. The contact area between the fibre, glue, and packaging needs to be taken into consideration.

Fig. 9. The bending of PTFE material on one-sided packaging (color online)

Meanwhile, the result of two-sided packaging is shown in Fig. 8(b). The best results are in the 1 and 2 mm packaging thickness, but they have not reached the simulation result. Similar to one-sided packaging, the linearity in other thickness does not cover the expected range of 100 °C. The 10 mm thickness does not respond to temperature change, which opens to whole other application of optical fibre sensor where temperature effect is to be eliminated, for example as temperature-insensitive strain sensor.

From Table 4, it can be seen that the packaging thickness cannot be simulated yet, as the simulation is only based on axial strain and the heat was assumed to be uniformly distributed. It comes as a consideration while designing the packaging dimension because packaging thickness is related to heat distribution, therefore this aspect could be considered for future research. From the data in Table 4, it can also be inferred that thin packaging gives more sensitive, fast, and sometimes unsteady responses, while thick packaging can store heat inside the material so the response can be too slow and cannot provide an accurate measurement.

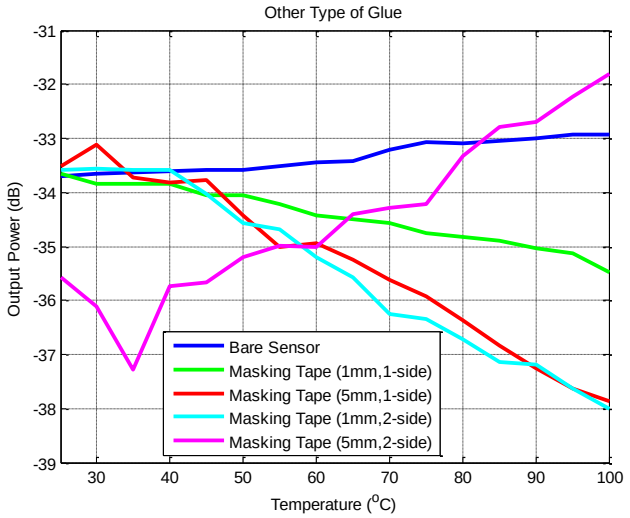

Fig. 10. Experiment results: the output response of the SMS fibre structure temperature sensor using masking tape as glue and various packaging thickness (color online)

The results in Table 4 also have a different measurement range, caused by the usage of different SMS sensor for different packaging thickness. The usage of one SMS structure for every type of packaging is not possible since epoxy resin is a permanent glue. The proposed solution is using impermanent glue where in this research masking tape is used. The result of this experiment is shown in Fig. 10 and Table 5.

Table 5. The sensitivity of PTFE-packaged SMS fibre temperature sensor with masking tape as glue

Type of glue	Thickness	Sensitivity (dB/°C)
Bare Sensor	-	0.0103
Masking tape (one-sided packaging)	1 mm	-0.0244
	5 mm	-0.0579
Masking tape (two-sided packaging)	1 mm	-0.0590
	5 mm	0.0501

As shown in Fig. 10, the sensor with two-sided packaging, 1 mm thickness, and masking tape as glue has the best response. The sensor has the sensitivity of -0.0590 dB/°C, about 5.7 times higher than the bare sensor. It is not as high as the simulation results shown in section 3.1. For the one-sided packaging, both thicknesses result in the increased sensitivity of the sensor, but fluctuating result in 5 mm thickness. The last sensor, the 5 mm two-sided packaging, give an unexpected result with positive gradient, different from both other experiments and the simulation. Overall, the experiment using masking tape has better linearity compared to those using epoxy resin.

Possible future research is to find the best combination of packaging material, thickness, glue material, and possibly, the shape of the packaging. Besides the thermal properties of packaging material, it is advised to consider the mechanical properties, for the strain cannot be overlooked while designing a temperature sensor. For example, a portion of the strain from thermal expansion is absorbed by the packaging when the strain transfers from the packaging to the fibre core, and hence only a segment of structural strain is sensed. The percentages can be stated as strain transfer efficiency. It is found from the theoretical analysis [35] that the strain transfer characteristics of fibre sensors depend on the mechanical properties of the cladding, the packaging, and the gauge length of the fibre sensor embedded in the structures subjected to strain. Also, non-uniform strain distribution caused by the shortage of bonded length between materials, which can be reduced by selecting proper adhesive/glue [36].

b. Wavelength shift method

The experiment to obtain wavelength shift is done to bare sensor and one selected sensor, the two-sided 1 mm packaging with masking tape as glue. The result is shown in Fig. 12. In the experiment, there was not enough data points to achieve similar graph as the simulation. The wavelength shift is examined for limited temperature rise from 25 °C to 30 °C. The lowest peak shifts to the longer wavelength when the bare sensor is exposed to temperature rise, from λ=1558,04 nm to 1564,66 nm.

Meanwhile, in the PTFE-packaged sensor, the lowest peak shifts to lower wavelength, λ=1538,31 nm. The sensitivity of the sensor is manually calculated from the wavelength peak shift. For bare sensor, the estimated sensitivity is 1.324 nm/°C, while for PTFE-packaged sensor is -3.946 nm/°C. The experiment also shows that the application of packaging changes the shape of the output spectrum. There is power intensity difference between bare sensor and packaged sensor even when there is no temperature difference.

The experiment results are very large compared to the simulation results. The sensitivity of PTFE-packaged sensor is -3946 pm/°C, while the simulation result -223,35 pm/°C. The limitation of the spectrum detector used in this experiment is the cause. The resolution of the device is ±6.6 nm, so that there is only 15 data points for wavelength range of 1500-1600 nm. The data cannot accurately show the spectrum, compared with the simulation where the resolution is 1 pm. However, the trend proves that there are wavelength shifts for SMS optical fibre in response of temperature change, and the results agree with previous reports that states the increased sensitivity after the use of PTFE packaging.

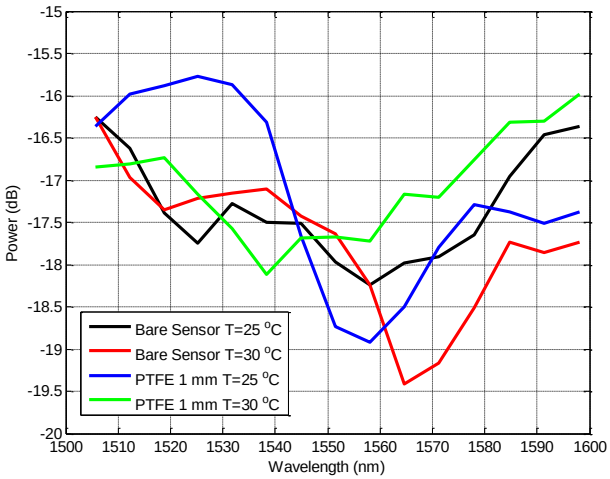

Fig. 11. Experiment results: the output response of the SMS fibre structure temperature sensor using masking tape as glue and various packaging thickness (color online)

4. Conclusions

PTFE packaging scheme for a singlemode-multimode-singlemode (SMS) fibre structure as a temperature sensor has been investigated. The packaging materials increase the sensitivity of the sensor differently based on the CTE of material. The length of MMF section is 43-mm, while thickness variations of packaging are 1, 2, 3, 5, 6, and 10 mm. The simulation in intensity-based measurement shows how PTFE application as packaging increases the sensitivity from 0.0110 dB/°C to -0.1050 dB/°C, about 9.4 times higher. Meanwhile in experiment, the sensor with two-sided packaging, 1 mm thickness, and masking tape as glue has the best response. The sensor has the sensitivity of -0.0590 dB/°C, about 5.7 times higher than the bare sensor which is 0.0103 dB/°C. Using the wavelength shift method, similar result is obtained where PTFE as packaging delivers the largest increase in sensitivity compared to other materials.

Acknowledgement

This work was supported by the Directorate of Research and Community Service, Ministry of Research, Technology, and Higher Education, Republic of Indonesia [Contract No: 26/PKS/ITS/2019].

References

[1] R. Xing, C. Dong, Z. Wang, Y. Wu, Y. Yang, S. Jian, Optics and Laser Technology **102**, 17 (2018).

[2] E. Li, G.-D. Peng, Optics Communications **281**, 5768 (2008).

[3] Y. Li, Z. Liu, S. Jian, Photonics Sensor **4**(1), 21 (2014).

[4] Y. Zhao, X. G. Li, F. C. Meng, Z. Zhao, Sensors and Actuators, A: Physical **124**, 163 (2014).

[5] T. B. Waluyo, D. Bayuwati, Journal of Physics: Conf. Series **817**(012035), 1 (2016).

[6] M. Yasin, S. Harun, Kusminarto, Karyono, Warsono, A. Zaidan, H. Ahmad, J. Optoelectron. Adv. M. **11**(3), 302 (2009).

[7] O. S. Wolfbeis, Analytical Chemistry **76**, 3269 (2004).

[8] N. Sabri, S. A. Aljunid, M. S. Salim, R. B. Ahmad, R. Kamaruddin, Journal of Physics: Conference Series no. 012064, 423 (2013).

[9] A. Messica, A. Greenstein and A. Katzir, Applied Optics **35**(13), 2274 (1996).

[10] Y. C. Kim, W. Peng, S. Banerji, K. S. Booksh, Optics Letter **30**, 2218 (2005).

[11] A. D. Kersey, M. A. Davis, H. J. Patrick, M. Leblanc, K. P. Koo, C. G. Askin, M. A. Putnam, E. J. Friebele, Journal of Lightwave Technology **15**, 1442 (1997).

[12] Q. Wang, G. Farrell, Optics Letters **31**, 317 (2006).

[13] Y. Zhao, Y. Liao, Optics and Lasers in Engineering **41**, 1 (2004).

[14] S. M. Tripathi, A. Kumar, R. K. Varshney, Y. B. P. Kumar, E. Marin, J.-P. Meunier, Journal of Lightwave Technology **27**(13), 2348 (2009).

[15] P. Wang, H. Zhao, X. Wang, G. Farrell, G. Brambilla, Sensors **18**(858), 1 (2018).

[16] Y. Sun, D. Liu, P. Lu, Q. Sun, W. Yang, S. Wang, L. Liu, J. Zhang, IEEE Sensors Journal **17**(10), 3045 (2017).

[17] Q. Wu, A. M. Hatta, P. Wang, Y. Semenova, G. Farrell, IEEE Photonics Technology Letters **23**(2), 130 (2011).

[18] A. M. Hatta, K. Indriawati, T. Bestariyan, T. Humada, Sekartedjo, Photonic Sensor **3**(3), 262 (2013).

[19] A. Mufarrikha, A. M. Hatta, Sekartedjo, Proc. of SPIE. **944410**, 1 (2014).

[20] Y. Chen, Y. Wang, R. Chen, W. Yang, H. Liu, T. Liu, Q. Han, IEEE Sensors Journal **16**(2), 331 (2016).

[21] Y. B. Lin, K. C. Chang, J. C. Chern, L. A. Wang, IEEE Sensors Journal **5**(3), 419 (2005).

[22] Y. Zhang, X. Tian, L. Xue, Q. Zhang, L. Yang, B. Zhu, IEEE Photonics Technology Letters **25**(6), 560 (2013).

[23] U. Dreyer, K. D. M. Sousa, J. Somenzi, I. D. L. Junior, V. D. Oliveira, H. J. Kalinowski, Journal of Microwaves, Optoelectronics and Electromagnetic Applications **12**(2), 638 (2013).

[24] A. K. Chotimah, A. M. Hatta, D. Y. Pratama, Proc. of SPIE. **10150**, 1 (2016).

[25] Y. Zhang, L. Xue, T. Wang, L. Yang, B. Zhu, Q. Zhang, IEEE Sensor Journal **14**(4), 1143 (2014).

[26] L. J. Song, G. Q. Yu, Second International Conference on Communication Systems, Networks and Applications **1**, 67 (2010).

[27] D. Samiappan, A. V. S. Kesarikiran, V. Chakravartula, C. R. U. Kumari, K. Shubham, B. Aakash, R. Kumar, Wireless Personal Communications **110**, 593 (2019).

[28] P. S. Reddy, R. L. N. S. Prasad, D. Sengupta, M. S. Shankar, K. Srimannarayana, J. Optoelectron. Adv. M. **12**(10), 2040 (2010).

[29] Q. Yu, Y. Zhang, Y. Dong, Y. P. Li, C. Wang, H. C. Chen, 2012 Symposium on Photonics and Optoelectronics, Shanghai, China nr. 12948294 (2012).

[30] Q. Wang, G. Farrell, W. Yan, Journal of Lightwave Technology **26**(5), 512 (2008).

[31] E. Li, Optics Letters **32**(14), 2064 (2007).

[32] E. ToolBox, "Thermal Conductivity of some selected Materials and Gases," 2003. [Online]. Available: https://www.engineeringtoolbox.com/thermal-conductivity-d_429.html. [Accessed 27 January 2021].

[33] W.-H. Wang, Y.-J. Feng, W.-Q. Shi, Z.-Y. Xiong, S.-D. Li, W. Wu, J.-X. Lin, Proc. of SPIE, Shanghai, China nr. 18735378 (2009).

[34] R. K. Kirby, Journal of Research of the National Bureau of Standards **57**(2), 91 (1956).

[35] H.-N. Li, G.-D. Zhou, L. Ren, D.-S. Li, Journal of Engineering Mechanics **135**(12), 1343 (2009).

[36] J. Zhou, Z. Zhou, D. Zhang, Journal of Intelligent Material Systems and Structures **21**, 1117 (2010).

*Corresponding author: rima_adiati@apps.ipb.ac.id
amhatta@ep.its.ac.id